Zika Virus Envelope Protein forms disulfide bond-dependent polymers in connection with a persistent ER stress in A549 cells

Jonathan Turpin †, Etienne Frumence †, Wissal Harrabi, Chaker El Kalamouni, Philippe Desprès, Pascale Krejbich-Trotot *, Wildriss Viranaïcken *

Université de La Réunion, INSERM UMR 1187, CNRS 9192, IRD 249, PIMIT, Processus Infectieux en Milieu Insulaire Tropical, Plateforme CYROI, 2, rue Maxime Rivière, 97490 Sainte-Clotilde, Ile de La Réunion. France.

*Correspondence: wildriss.viranaicken@univ-reunion.fr (W.V.); pascale.krejbich@univ-reunion.fr (P.K.T.); Tel.: +33-262938829

† Contribute equally to this work.

Abstract: Flaviviruses replicate in membranous factories associated with the endoplasmic reticulum (ER). Significant levels of flavivirus polyprotein integration contribute to ER stress and the host cell may exhibit an Unfolded Protein Response (UPR) to this protein accumulation, stimulating appropriate cellular responses such as adaptation, autophagy or cell death. These different stress responses support other antiviral strategies initiated by infected cells and can help to overcome viral infection. In epithelial A549 cells, a model currently used to study the flavivirus infection cycle and the host cell responses, all three pathways leading to UPR are activated during infection by Dengue virus (DENV), Yellow Fever virus (YFV) or West Nile virus (WNV). In the present study, we investigated the capacity of ZIKA virus (ZIKV) to induce ER stress in A549 cells. We observed that the cells respond to ZIKV infection by implementing an UPR through activation of the IRE1 and PERK pathway without activation of the ATF6 branch. By modulating the ER stress response, we found that UPR inducers significantly inhibit ZIKV replication. Interestingly, our findings provide evidence that ZIKV could manipulate the UPR to escape this host cell defence system. Since incomplete UPR could lead to unresolved and persistent ER stress, we found that ZIKV infection was associated with an abnormal accumulation of viral envelope proteins, which were aggregated with non-native disulfide bridges. As the presence of these “amyloid like” protein polymers may be cytopathic, our observations provide new insights into specific neuropathologies associated with ZIKA virus infections.

Keywords: Zika virus; Unfolded Protein Response; Persistent ER stress; Aggregate; Non-native disulfide bond.

1. Introduction

ZIKA virus (ZIKV) is a pathogenic single-stranded RNA virus belonging to the Flaviviridae family together with DENV, WNV and JEV. Among the pathogenic flaviviruses, ZIKV has gained notoriety in the last ten years, due to explosive outbreaks and serious clinical concerns. Neurological complications have been described, including Guillain-Barré syndrome (GBS) and congenital malformations, prompting specific vigilance for pregnant women in the event of a Zika epidemic [1,2]. Due to these atypical clinical manifestations, the ability of ZIKV to be transmitted sexually in addition to being vector-borne, and the evidence of its persistence in some tissues, increasing numbers of molecular and cellular studies investigate specific ZIKV-host interactions that distinguish it from the other flaviviruses. Similar to other flaviviruses, ZIKV replication occurs in Endoplasmic Reticulum (ER) invaginations of infected cells and leads to an accumulation of viral proteins [3–5]. Genome translation is followed by proteolytic cleavage of the polyprotein into three structural (C, M, and E) and seven non-structural (NS1, NS2A, NS2B, NS3, NS4A, NS4B, and NS) proteins which are incorporated into the ER membrane.

Preprints (www.preprints.org) | NOT PEER-REVIEWED | Posted: 6 December 2019 doi:10.20944/preprints201912.0084.v1

The ER is thus an essential cellular compartment for the completion of the viral cycle, in addition to several key mechanisms in cell physiology. The standard function of the ER is to regulate folding and post-translational modification of proteins that are to be transported within the cell, or secreted. The correct folding of the proteins depends on the N-linked protein glycosylation, the oxidative environment in the ER lumen which promotes the formation of disulfide bonds, and the presence of several Ca2+-dependent molecular chaperones (calreticulin, GRP78 also named BiP and GRP94) which stabilize protein folding intermediates [6,7]. ER homeostasis can be perturbed in the case of glucose starvation, hypoxia, calcium dysregulation or following a protein accumulation which will in turn provoke ER stress. The Unfolded Protein Response (UPR) is activated in response to ER stress, in an attempt to restore ER homeostasis. In cells infected by a virus, the huge and sudden accumulation of viral proteins that are processed in the ER usually results in ER stress and the induction of the UPR. This cell response has been shown to be involved in several modes of cell defence, i.e. antiviral programs, immune responses [8,9] and commitment in autophagy or cell suicide [10,11]. During ER stress, the folding chaperone GRP78/BiP dissociates from three ER-resident transmembrane proteins i.e. PKR-like endoplasmic reticulum kinase (PERK), Inositol-Requiring Enzyme 1 (IRE1) and activating transcription factor 6 (ATF6) [12]. Each of these proteins acts as a stress transducer in independent pathways devoted to stress resolution. The activated kinase activity of PERK results in phosphorylation of eIF2α, followed by a transitory translational attenuation and consequently reduced ER influx of newly synthesized proteins. The endonuclease activity of activated IRE1 produces a spliced form of the x-box binding protein 1 (Xbp1) transcript. This spliced Xbp1 encodes a transcription factor that promotes the expression of genes coding for several factors aimed at resolving ER stress. ATF6 is soluble and can egress from the ER to the Golgi apparatus for maturation by S1P or S2P cleavage to generate ATF6f. ATF6f acts in the nucleus where it regulates UPR target gene expression. The transcriptional activity of ATF6 and Xbp1 leads to increased expression of chaperones and proteins implicated in enhanced folding capacity or in ER-associated protein degradation (ERAD). In spite of the implementation of a UPR with these adaptive mechanisms, an excessive, unresolved or prolonged ER stress will result in cellular autophagy or apoptosis [13]. Crosstalk between ER stress, UPR, autophagy and apoptosis pathways are of particular importance in the case of virally infected cells since each of these responses will influence the infected cell's health and contribute to determining the efficacy of the viral replication and spread.

It has previously been shown that ZIKV has the ability to initiate a UPR response to ER stress in several cell types [14–18] (Table 1) and that infection is accompanied by morphological modification of cellular organelles [19]. However, it is important to decipher how ER stress initiation is mediated, which branches of the UPR pathways are involved and how pathway crosstalk is mediated during cellular and ER responses to ZIKV infection. In epithelial A549 cells, a widely *in vitro* used cell line to characterize cell responses to flavivirus infection (DENV, WNV, JEV), all three branches of the UPR are activated (PERK, ATF6 and IRE1) and associated with enhanced GRP78/BiP expression [20–23]. In this present work, we followed ER stress and the UPR in A549 cells in order to identify mechanisms that could be specific to ZIKV infection and that may lead to new "*in cellulo*" approaches for understanding clinical outcomes. Imaging of infected cells and detection of an insoluble fraction of viral proteins strongly suggested a long lasting ER stress. When we looked at the stress transduction mechanisms, we discovered that the UPR was initiated by the host cell but with no activation of the ATF6 branch. This was unexpected regarding previous observations with other flaviviruses including DENV, JEV and WNV [21,23,24]. Considering that UPR pre-activation can limit ZIKV infectious capacity [9], we hypothesized that a partial or impaired UPR could be beneficial for the virus and showed that exogenously-induced UPR was also detrimental to ZIKV at the post entry step. ZIKV would thus have the ability to modulate UPR to its benefits with a mechanism that remains to be discovered. Moreover, this control with unresolved and prolonged ER stress was characterized by the production of significant proportions of oxidized viral E proteins (E-ZIKV). This new data suggests that an accumulation of E-ZIKV protein

organized into insoluble non-native disulfide bonded polymers could be responsible for proteinopathies and could therefore contribute to the neuropathological disorders associated to ZIKA virus infections during the 2015-2016 south-american outbreak.

2. Materials and Methods

2.1. Virus, Cell culture, antibodies and reagents

The clinical isolate PF-25013-18 (PF13) of ZIKV [25] was used for all infections. A549 cells (ATCC, CCL-185) were cultured at 37 °C under a 5% CO2 atmosphere in MEM medium supplemented with 10% heat-inactivated foetal bovine serum (FBS). Plaque assays were used for viral progeny quantification as described previously [26]. Cell damages were evaluated measuring lactate dehydrogenase (LDH) release resulting from a plasma membrane rupture. Supernatants of infected cells were collected and subjected to a cytotoxicity assay, performed using CytoTox 96® non radioactive cytotoxicity assay (Promega) according to manufacturer instructions. Absorbance of converted dye was measured at 490 nm using a microplate reader (Tecan).

Immunodetection of the viral proteins was performed using the mouse anti-pan flavivirus envelope E protein mAb 4G2, produced by RD Biotech, or with the rat anti-EDIII ZIKV wich was described previously [27]. The rabbit anti-Calnexin antibody was purchased from Santa-Cruz Biotechnology (Clinisiences, Nanterre, France). Donkey anti-mouse Alexa Fluor 488 and anti-rabbit Alexa Fluor 594 IgG antibodies were from Invitrogen (Thermofisher, Les Ulis, France). Horseradish peroxidase-conjugated anti-rabbit (ab97051) and anti-mouse (ab6789) antibodies were from Abcam (Cambridge, UK). The antibody against GRP78/Bip (#3177) was from cell Signalling Technology (Ozyme, Saint-Cyr-l'École, France). Thioflavin T, a benzothiazole dye that increases in fluorescence upon binding to amyloid fibrils and protein aggregates was purchased from Sigma-aldrich (Humeau, La Chapelle-Sur-Erdre, France). Thapsigargin (TG), an endoplasmic reticulum Ca^{2+}-ATPase inhibitor and Tunicamycin (TM) an inhibitor of N-glycosylation were used to induce ER stress and UPR respectively at 1 µM and 2 µg.mL^{-1} for the indicated time in figure legends. These inhibitors were from Sigma-aldrich (Humeau, La Chapelle-Sur-Erdre, France).

2.2. Luciferase Reporter assay

Plasmids with GRP94 and GRP78 promoters upstream of F-Luc (pGRP78-Luc and pGRP94-Luc) were provided by Dr. Kazutoshi Mori [28]. One million cells were transfected with the indicated plasmids using Lipofectamine 3000 according to manufacturer instructions (Invitrogen, Thermofisher, Les Ulis, France), incubated for 12 h and then divided into three separate flasks. The first flask was mock treated, the second was infected with ZIKV PF13 at MOI of 5 for 24h and the third was treated with thapsigargin (1µm) for 6 hours. Luciferase activities were measured using the Luciferase Glo™ assay according to manufacturer's instructions (Promega, Madison, USA).

2.3. Cell fractionation and Western blot

For fractionation, cells were washed with PBS and lysed at the concentration of 1x10^4 cells.µl^{-1} in buffer A (0.2% Triton X-100, 50 mM Tris-HCl pH 7.5, 150 mM NaCl, 2.5 mM EDTA) as before [29]. The Triton X-100-insoluble fraction was separated by centrifugation at 3400 g for 10 min. Pellets were enriched in non-folded proteins and the supernatant enriched in Triton X-100 soluble proteins. All fractions were used in western blots.

For the rest of the study, proteinaceous extracts were prepared by harvesting cells in RIPA buffer after two washes with PBS. Cells were sonicated and protein extracts were treated in Laemmli buffer with DTT and boiled at 95°C for 5 min.

2.4. Immunofluorescence and thioflavin T staining

A549 cells were grown, infected or treated on glass coverslips. They were further fixed with 3.7% formaldehyde at room temperature for 10 min. Fixed cells were permeabilized with 0.1% Triton X-100 in PBS for 5 min. Coverslips were incubated with primary antibodies (1:1000 dilution) in 1x PBS 1% BSA for two hours and with Alexa Fluor-conjugated secondary antibodies (1:1000, Invitrogen) for one hour. Nucleus morphology was revealed by DAPI staining. According to Beriault and Werstuck [30], ER stress indicator thioflavin T was added to the coverslips at 5µM after immunodetection of calnexin or ZIKV E DIII and DAPI staining, for 10 min and directly mounted. The coverslips were mounted with VECTASHIELD® (Clinisciences, Nanterre, France) and fluorescence was observed using a Nikon Eclipse E2000-U microscope. Images were captured and processed using a Hamamatsu ORCA2 ER camera and the imaging software NIS-Element AR (Nikon, Tokyo, Japan).

2.5. RT-PCR

Semi quantitative RT-PCR experiments were performed as before [22]. Primers used for RT-PCR were CHOP: F 5'-GCACCTCCCAGAGCCCTCACTCTCC-3′, R 5′-GTCTACTCCAAGCCTTCCCCCTGCG-3′; GRP78: F 5′-CATCACGCCGTCCTATGTCG-3′, R 5′-CGTCAAAGACCGTGTTCTCG-3′; XBP1: F 5'-CCTTGTAGTTGAGAACCAGG-3', R 5'-GGGGCTTGGTATATATGTGG-3'; NS1: F 5′-AGAGGACCATCTCTGAGATC-3', R 5′-GGCCTTATCTCCATTCCATACC-3'; GAPDH: F 5′-GGGAGCCAAAAGGGTCATCA-3', R 5′-TGATGGCATGGACTGTGGTC-3'. PCR products were analyzed on a 1.5% agarose gel electrophoresis and stained as described before [19].

2.6. Statistical analysis

All values are expressed as mean ± SD of at least three independent experiments, as indicated in the figure legends. After normality tests, comparisons between different treatments were analyzed using a one-way ANOVA. Values of $p<0.05$ were considered statistically significant for a post-hoc Tukey's test. All statistical tests were done using the software Graph-Pad Prism version 7.01.

3. Results and discussion

A549 epithelial cells have been shown to be permissive to infection by most flaviviruses [25,31] and are a suitable model for studying *in cellulo* host-virus interactions. Many research teams, including ours, have used this epithelial cell line to characterize ZIKV infection with different strains of the epidemic (clinical isolate PF13, molecular clone BR15) and historical (MR766) ZIKV, deciphering viral entry pathways, viral replication kinetics [32] and cellular responses such as apoptosis [33]. As protein load increases in cells replicating the virus resulting in the accumulation of misfolded or partially processed viral polyproteins and ER stress, we investigated markers of ER stress and the contribution of the Unfolded Protein Response during the course of ZIKV infection.

3.1. ZIKV infection induces ER morphological changes associated with enhanced Thioflavin T fluorescence and accumulation of misfolded and insoluble forms of E-ZIKV protein.

When stressed, the ER exhibits morphological abnormalities with luminal swelling and membrane expansion [34]. These morphological changes can be observed by fluorescence microscopy. When we compared Calnexin expression, a standard ER marker, between A549 cells infected for 48hours with the epidemic strain of ZIKV (PF13) and control (mock infected cells), we noticed morphological shape changes of the ER with obvious swelling and increased calnexin staining (Figure 1). Imaging of the infected cells also showed the colocalization of

Preprints (www.preprints.org) | NOT PEER-REVIEWED | Posted: 6 December 2019 doi:10.20944/preprints201912.0084.v1

immunodetected viral envelope protein (E-ZIKV) and calnexin, confirming that viral proteins are present in the enlarged and globe-shaped compartment of an expanding ER (Figure 1).

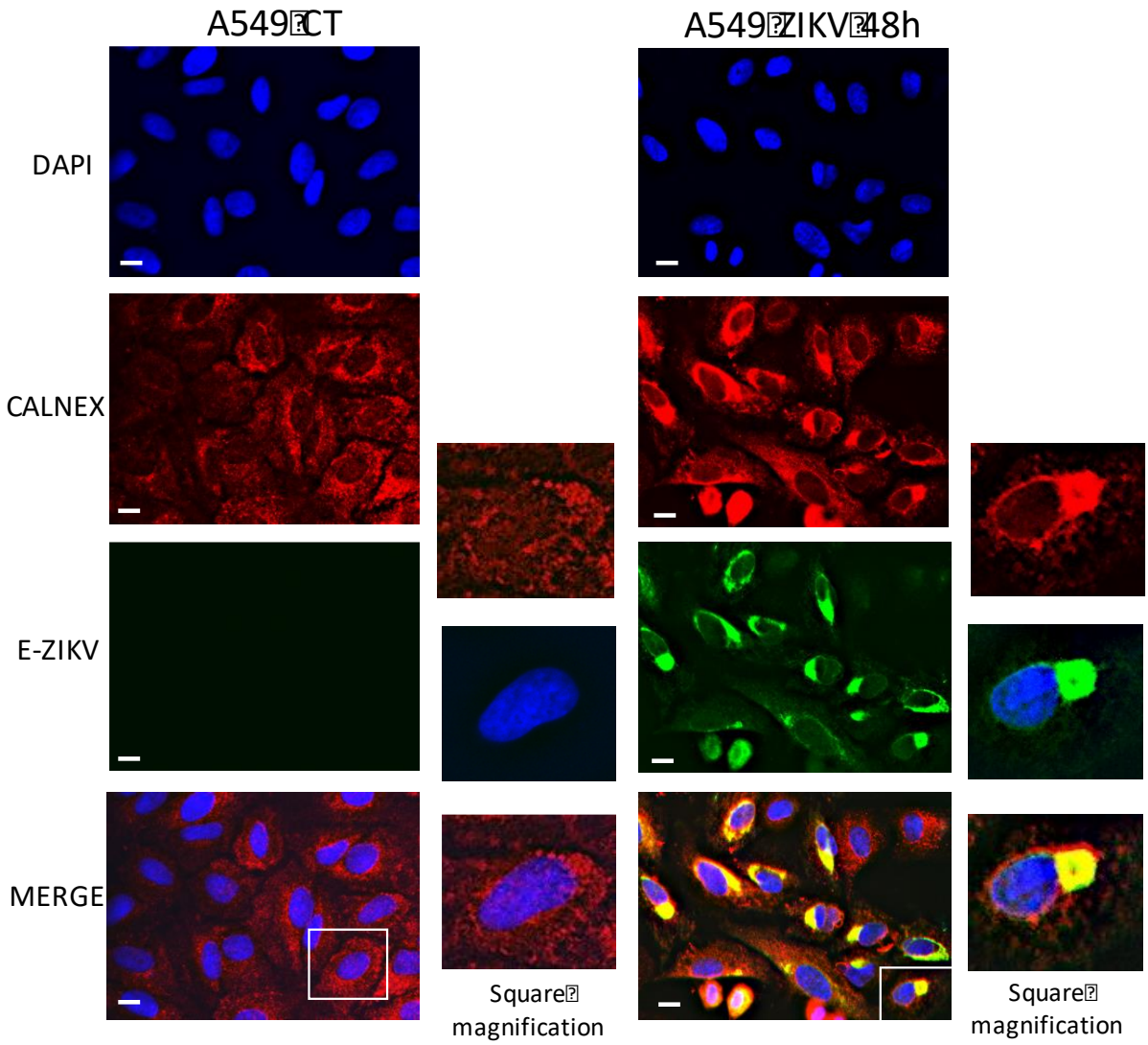

Figure 1. ER morphological features during ZIKV infection.

A549 cells were infected with ZIKV at MOI of 1 for 48h. Cells were immunostained for calnexin and E-ZIKV. Scale bar: 5 µm. Right panel series show magnified details of a selected cell from the x200 microscopic field (white square). All experiments were representative of three independent experiments.

Thioflavin T, a small fluorescent molecule that binds selectively to beta sheets and aggregated proteins gave a strong fluorescent signal, binding readily to the malformed ER expressing E-ZIKV in the infected cells (Figure 2A). This dye has been described as an effective tool for the detection of accumulated protein aggregates that are symptomatic of ER stress [30]. In order to better characterize the underlying cause of this high signal obtained with thioflavin T, we looked at the envelope (E-ZIKV) protein accumulation and signs of associated misfolding. Using cell fractionation, as described previously for ERGIC-53 proteins (belonging to ER), we separated soluble and insoluble proteins [22] and measured the distribution of E-ZIKV between these two fractions (Figure 2B). Detection of E-ZIKV with an antibody raised against domain III of the E protein (EDIII) revealed an accumulation of insoluble forms (i.e. unfolded) of E-ZIKV. This data support ER stress induction upon ZIKV infection in A549 cells.

Preprints (www.preprints.org) | NOT PEER-REVIEWED | Posted: 6 December 2019 doi:10.20944/preprints201912.0084.v1

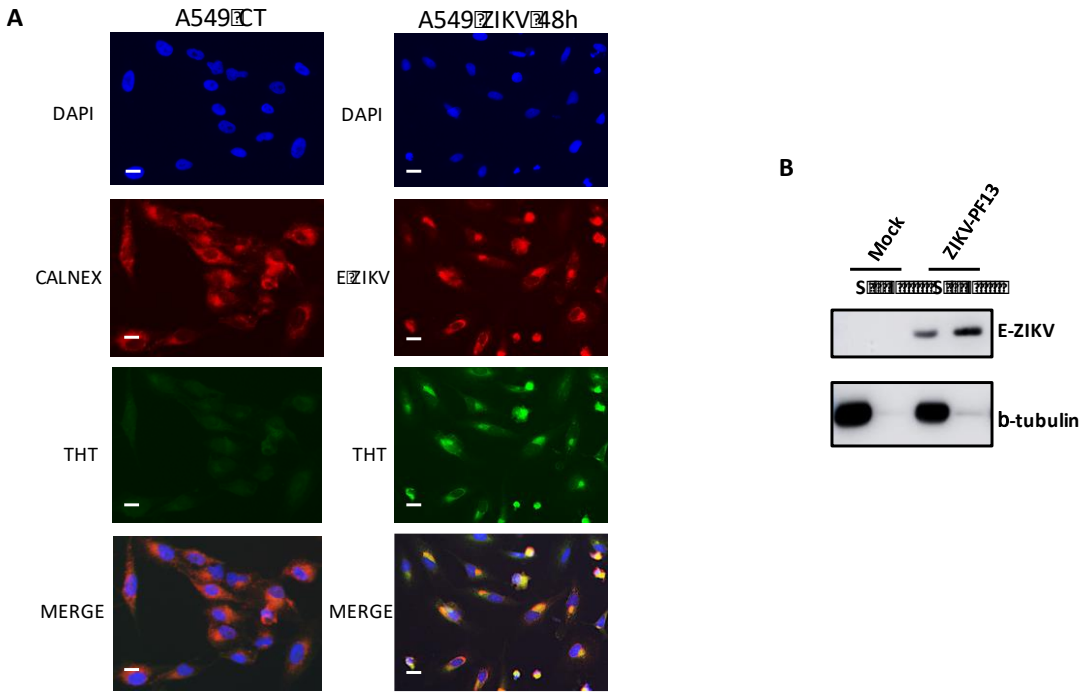

Figure 2. ZIKV infection is associated with accumulation of unfolded protein and insoluble E-ZIKV. (A) A549 cells infected with ZIKV at MOI of 1 for 48h were incubated with Thioflavin T (THT), a fluorescent ER stress indicator that binds aggregated proteins. Infected cells were counterstained with E-ZIKV Scale bar: 5 µm. **(B)** A549 cells were infected with ZIKV at MOI of 5. 48h post-infection cells were lysed in TX100 buffer A. An equal volume of total (T), soluble (S) and insoluble (I) fractions were separated under reducing conditions and immuno-blotted for E-ZIKV with anti-EDIII antibody. All experiments were representative of three independent experiments.

3.2. Unfolded Protein Response during ZIKV infection in A549 cells

Upon ER stress, cells initiate an UPR to prevent persistent damage due to stress and to restore ER homeostasis. In order to decipher the stress transduction mechanisms induced upon ZIKV infection in A549 cells, we analyzed each of the three main UPR pathways. For this purpose, we investigated the expression level of target genes specific to each activated branch.

3.2.1. Effect of ZIKV infection on PERK and IRE1 pathways of UPR.

Activation of the PERK pathway results in eIF2α phosphorylation which is followed by a reduced translation rate. It also leads to ATF4 upregulation. ATF4 is a transcription factor acting on several targets among which is the C/EBP homologous protein (CHOP) encoding gene. CHOP factor plays a key role in stress resolution and in relationships between UPR, cell survival or cell death. We therefore followed activation of this PERK/ATF4 branch by a measure of the expression level of the CHOP gene by RT-PCR (Figure 3A). Effective upregulation of CHOP at the transcriptional level suggests that the PERK branch of UPR was activated during ZIKV infection of A549 cells. This observation is in agreement with previous findings in ZIKV infected human neural stem cells [14].

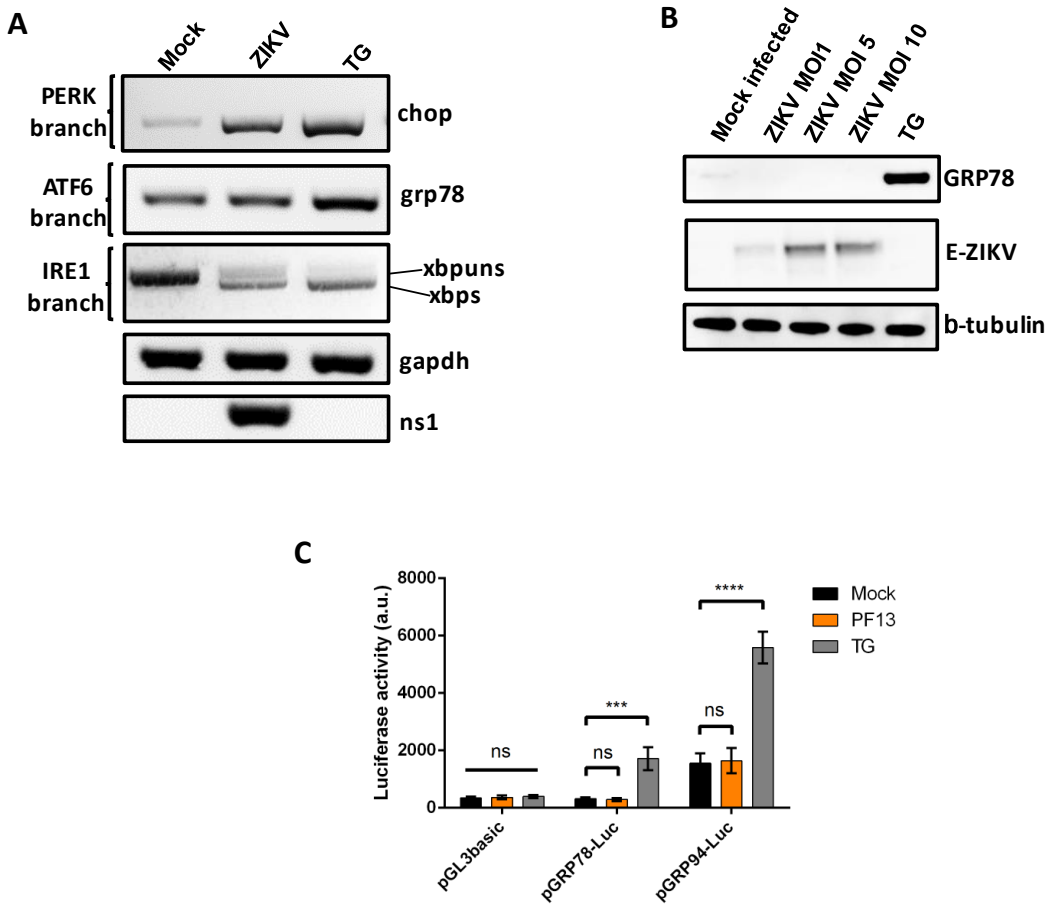

Figure 3. UPR branch activation during ZIKV infection. (A) A549 cells were infected with ZIKV at MOI of 1 for 24h. RT-PCR were performed to monitor transcriptional regulation of downstream gene targets of the UPR branch, chop (PERK branch), Xbp1 splicing (IRE1 branch) and grp78 (ATF6 branch). u-Xbp1 correspond to unspliced Xbp1 and s-Xbp1 to spliced Xbp1. **(B)** A549 cells infected with ZIKV at indicated MOI for 48h were lysed in buffer A, total protein extracts, under reducing conditions were immuno-blotted for E-ZIKV with EDIII antibody, GRP78 and β-tubulin as a loading control. **(C)** A549 cells ($1x10^6$ cells) were transfected with the indicated reporter constructs. After 12h, transfected cells were plated at a density of $3x10^4$ cells per well and infected with ZIKV at MOI of 5. Luciferase activities were measured 24h post infection. Degrees of significance are indicated in the figure captions as follow: * $p < 0.05$; ** $p < 0.01$; *** $p < 0.001$, **** $p < 0.0001$, ns = not significant. For all experiments Thapsigargin-ER stress induced (TG) were used as positive control at 1 µM for 6h. RT-PCR and western blot experiments were representative of three independent experiments.

The IRE1 pathway is characterized by the splicing of the Xbp1-transcript. The spliced Xbp1 (s-Xbp1) encodes a transcription factor able to transactivate genes mainly involved in ERAD. Splicing of Xbp1 was then followed by RT-PCR as an indicator of IRE1 branch activation. s-Xbp1 was detected upon ZIKV infection like in cells treated with thapsigargin (TG), an endoplasmic reticulum Ca^{2+}-ATPase inhibitor that is an ER stress and UPR inducer (Figure 3A). The observation of IRE branch activation by ZIKV was also in accordance with previous findings [10].

3.2.2. Effect of ZIKV infection on ATF6 branch of UPR

The third branch of the UPR is mediated by the maturation of ATF6 upon S1P or S2P processing in the Golgi apparatus. Once translocated to the nucleus, mature ATF6 upregulates

Preprints (www.preprints.org) | NOT PEER-REVIEWED | Posted: 6 December 2019 doi:10.20944/preprints201912.0084.v1

the expression of chaperone encoding genes like GRP78 (Bip) and GRP94. Increased levels of these chaperones, involved in the refolding of proteins, plays a crucial role in the resolution of ER stress. Unlike thapsigargin treatment of A549 cells, RT-PCR results revealed that grp78 was not upregulated at the transcriptional level during ZIKV infection (Figure 3A). This observation is potentially important as it could be one of the specific interactions of ZIKV that differentiates it from other flaviviruses. Indeed, until now, studies of the UPR response to flavivirus infections, such as for DENV, report the ability of the infected cells to induce grp78 transcription in this A549 model [22].

We further investigated this lack of GRP78 upregulation by two approaches. We first checked the GRP78 protein levels by western blot in cells that were infected for 48h at increasing ZIKV MOI (1, 5 and 10). No modulation of GRP78 expression could be detected under any of these conditions (Figure 3B). We noticed low or undetectable levels of the GRP78 protein while an RT PCR signal was obtained for the grp78 mRNA. Translational or post-translational regulation could be responsible for this signal discrepancy, or protein expression levels may have been below the limit of detection of out antibody system.

In a second approach, we monitored ATF6 activity using luciferase reporter constructs. We transfected A549 cells with plasmids encoding a F-Luc reporter gene downstream of grp78 or grp94 promoter. These two promoters contain the ER stress response element (ERSE) which is transactivated by ATF6. Thapsigargin induced expression of the F-Luc reporter gene under control of ERSE for both grp78 and grp94 constructs. This was not the case after ZIKV infection (Figure 3C).

Together these results suggest that ZIKV infection provides a partial transduction of the ER stress with activation of the PERK/ATF4 and IRE1 pathways of the UPR but without any involvement of ATF6. Incomplete or delayed re-folding chaperone induction due to this missing branch of UPR could impact the adaptive response and lead to persistent ER stress. This could also interplay with programmed cell death by signalling pathways downstream of PERK activation with CHOP-mediated regulation of proteins involved in apoptosis like BIM, Bcl-2 and PUMA [27].

3.3. Crosstalk between UPR and ZIKV

Given the ATF6-independent activation of the UPR during ZIKV infection (Figure 3) associated with the detection of aggregated proteins and insoluble forms of E-ZIKV (Figure 2A, 2B) and considering that ZIKV can delay apoptosis [25,33,35], we hypothesized that ZIKV infection could lead to a persistent and unresolved ER stress. We therefore investigated crosstalk between ZIKV and the UPR through exogenous induction of UPR following ZIKV infection.

3.3.1. UPR Affects ZIKV infection

ER stress can be induced by the action of tunicamicyn (TM), an inhibitor of N-glycosylation. The resulting UPR can be qualified as ‘standard’ with activation of the PERK, IRE1 and ATF6 pathways [30]. In order to see the effect of exogenous activation of UPR on ZIKV infection, we added this inducer to infected cells 2h after ZIKV inoculation. Cells were harvested and cell culture supernatant collected after 16h of treatment with TM. When we looked at the viral protein expression in cells, as an indicator of viral replication efficiency, we observed a dose dependent reduction of E-ZIKV following TM treatment (Figure 4A).

Preprints (www.preprints.org) | NOT PEER-REVIEWED | Posted: 6 December 2019 doi:10.20944/preprints201912.0084.v1

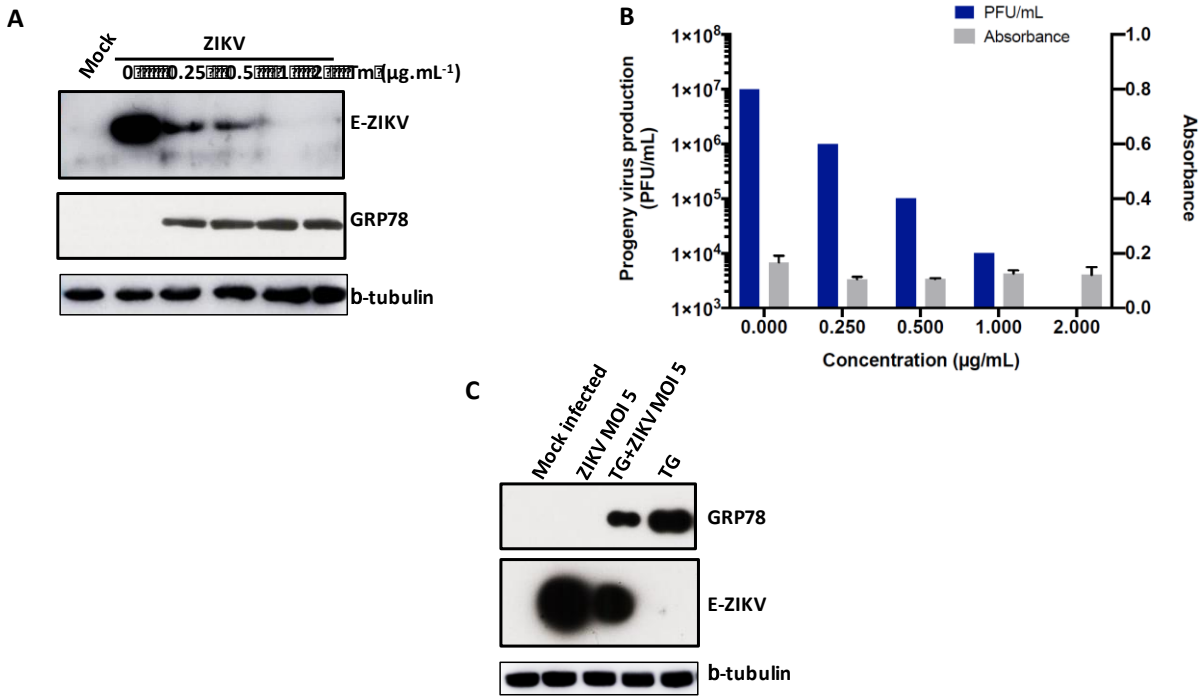

Figure 4. Crosstalk between UPR and ZIKV during infection. (A) A549 cells were infected with ZIKV at MOI of 5 for 18h. 2h post-infection tunicamycin (TM) was added at the indicated concentration. Total protein extract under reducing conditions were immuno-blotted for E-ZIKV with EDIII antibody, GRP78 and β-tubulin as a loading control. **(B)** Viral progeny production in cell culture supernatants of cells infected and treated with TM were determined by PFU assay (left axis). Cell mortality was evaluated through LDH release and absorbance measurement (right axis). **(C)** A549 cells were infected or not with ZIKV for 16h at MOI of 5, followed by 4h treatment with TG at 1µM. Western blot were performed on total extract as in (A). All results were representative of three independent experiments.

When we looked at the viral progeny production in cell supernatants, we found that this production was abrogated by the TM treatment in a dose-dependent manner (Figure 4B). To ensure that the observed effect was not be related to cell death upon infection or treatment, we controlled for the amount of released LDH in cell culture supernatants (Figure 4B). Using thapsigargin (TG), a UPR inducer that works by alteration of Ca^{2+} homeostasis, or dithiothreitol (DTT), a UPR inducer by that works by blocking disulfide bond formation, incubated with infected cells for 16 h, 2h after ZIKV inoculation, we observed the same inhibition of ZIKV infection (Figure S1). These observations suggest that a 'standard' UPR has the ability to interfere with ZIKV replication efficiency, independently of the nature of the UPR inducer and even after the post-entry step. This result complements previous findings that pre-activating the UPR response decreases flavivirus titers [9]. However, in the mentioned study, the antiviral effect of the UPR relied on an early activation, priming an IFN regulatory factor 3 dependant innate immune signalling. In our case, since the UPR inducer is added 2 hours after the virus, the mechanism that limits infection should be different and exerted on a virus cycle already in progress.

3.3.2. ZIKV Infection Modulates the ATF6 branch of UPR in A549 cells

As we found that ZIKV infection of A549 cells led to ER stress and UPR but with an impaired ATF6 branch with no GRP78 induction, we hypothesized that ZIKV could hijack this UPR branch and could take advantage of an unresolved ER stress. To test this hypothesis, we treated ZIKV infected cells with TG for 4h and analyzed GRP78 expression by WB (Figure 4C).

Preprints (www.preprints.org) | NOT PEER-REVIEWED | Posted: 6 December 2019 doi:10.20944/preprints201912.0084.v1

As mentioned above, we observed a reduction in E-ZIKV expression, even with a shorter treatment with the UPR inducer (4h of TG instead of 16h of TM treatment in figure 3A). We also confirmed that ZIKV infection was not able to upregulate GRP78 at the protein level. Furthermore, when we compared the TG treatment alone and in the presence of ZIKV, we found that the virus decreased the level of GRP78 protein induced by TG. All together these data favor our hypothesis that UPR affects ZIKV replication, but that the virus has acquired the ability to block partially this response. The interference with UPR can lead to unresolved and persistent ER stress.

4. Accumulation of oligomers of Oxidized E-ZIKV

Folding state and protein load in the ER lumen are biological reporters of ER stress, influencing UPR transduction and subsequent cell adaptation. A lack of chaperone activity and incorrect stress resolution will lead to increased misfolding and cellular protein accumulation. We therefore determined which forms of E-ZIKV could be found in infected cells. After separation under non-reducing conditions (Figure 5A), we observed that high molecular weight variants of the E-ZIKV proteins accumulated in the insoluble fraction of cell extracts. The E-ZIKV monomer (M) has a predicted molecular weight of 55kDa. The observed high molecular weight is consistent with oligomers of the protein (Oligomer, O). Oligomers were only detected with the antibody raised against the domainIII of E protein (EDIII). Conversely, immunodetection with 4G2, a pan-flavivirus antibody that binds a conformational epitope which overlaps the E protein fusion loop [24], revealed mainly a monomeric form of E-ZIKV in the soluble fraction (Figure 5A). These observations suggest that during ZIKV infection, E proteins are produced and accumulated in diverse forms corresponding to a soluble, native and folded form of the protein but also to oligomerized unfolded or misfolded proteins retained in an insoluble fraction.

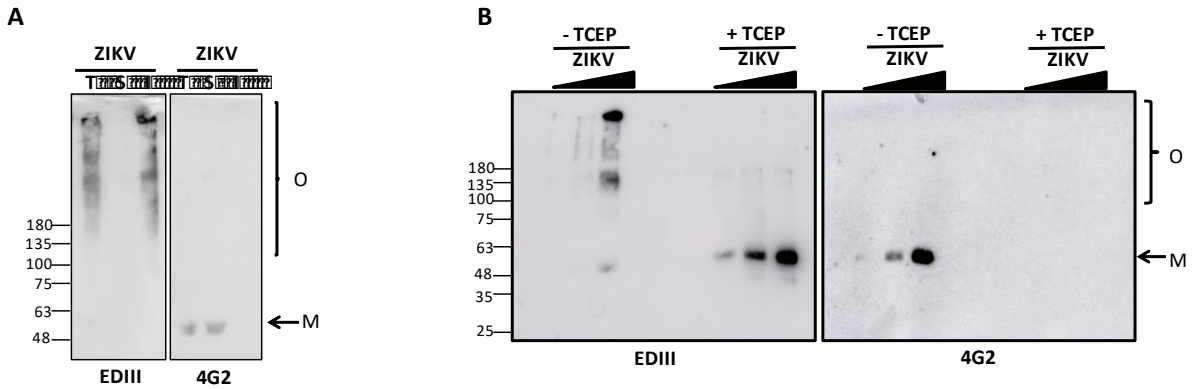

Figure 5. Accumulation of insoluble disulfide bonded oligomers of E-ZIKV. (A) A549 cells were infected with ZIKV at MOI of 5. 48h post-infection cells were lysed in TX100 buffer A. An equal volume of total (T), soluble (S) and insoluble (I) fractions were separated under non-reducing conditions and immuno-blotted for E-ZIKV with anti-EDIII or 4G2 antibody. M indicates the 55kDa monomer, O indicates high molecular mass oligomers of E-ZIKV **(B)** A549 cells were infected with increased quantities of ZIKV (MOI 0.5, 1 and 5) and total fraction were treated or not with TCEP before western blotting as in (B). Molecular weight marker was indicated on the left. All experiments were representative of three independent experiments.

As non-native disulfide bonds can prevent correct folding and require reduction or isomerization to form the correct, native disulfides bonds [36][25], we hypothesized that oligomers of E-ZIKV are due to non-native disulfide bonds formed between E-ZIKV monomers. Moreover, it is known that in case of unresolved and persistent ER stress, proteins can be oxidized, triggering non-native disulfide bonds responsible for oligomerization and aggregation. In the case of ZIKV infection with incomplete UPR activation, formation of these oxidized oligomers could be promoted and could contribute to maintain ER stress. To test this hypothesis, we treated cell protein extracts with Tris(2-carboxyethyl) phosphine (TCEP), a

Preprints (www.preprints.org) | NOT PEER-REVIEWED | Posted: 6 December 2019 doi:10.20944/preprints201912.0084.v1

reducing agent, and performed immunodetection of E-ZIKV as above. With the antibody raised against the EDIII, we were able to detect mainly oligomers under non-reducing conditions and monomers upon reduction with TCEP (Figure 5B). With the 4G2 antibody, only the monomeric form of E-ZIKV could be detected and the signal was lost in the presence of TCEP (Figure 5B). This observation argues in favour of a native folded E-ZIKV form that depends on intra-disulfide bonds. Conversely, unfolded or misfolded E-ZIKV would have led to disulfide bonded aggregates. Accumulation of this oligomerized forms of E-ZIKV during ZIKV infection also supports an effective redox imbalance in the ER leading to oxidation of E-ZIKV. To our knowledge, the observation of an accumulation of this type of aggregate during an infection by flaviviruses is quite new. In A549 cells infected with DENV, many studies report complete activation of the three branches of the UPR and no data support a persistence of ER stress [20]. However, we were unable to test whether DENV misfolding occurs by a similar mechanism as no antibody was available for such a test.

5. Conclusions

Our study showed that ZIKV infection of epithelial A549 cells could trigger ER stress through an accumulation of unfolded viral proteins. We confirmed the activation of the UPR in this cell model but that, unlike other flaviviruses [37], ZIKV does not activate all three branches of the UPR stress response (Figure 6). In addition, we found that the UPR can affect ZIKV cellular replication efficiency, but that ZIKV can interfere with a complete UPR. Therefore, we hypothesize that persistent ER stress is induced by ZIKV infection and exploited by the virus to increase its replication.

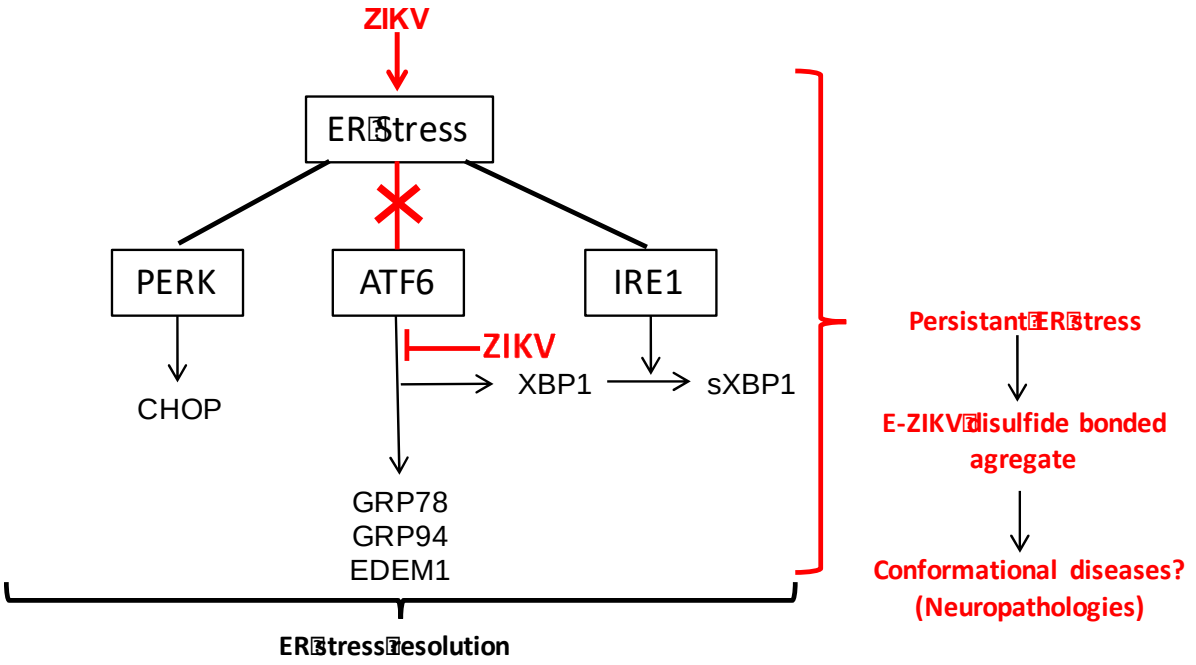

Figure 6. Schematic representation of the Unfolded Protein Response (UPR) upon ER stress and ZIKV interplay. This diagram summarizes the branches of the UPR and how ZIKV, by inducing an ER stress, modulates the response that is incomplete, leads to an accumulation of E-ZIKV disulfide bonded aggregates and persistent stress that could suggest mechanisms similarly involved in conformational diseases.

As ER dysfunctions combined with aggregated protein accumulation are responsible for neuronal degeneration in numerous human diseases, especially the ones related to proteinopathies and conformational diseases [38,39], we suggest that a virally orchestrated persistent ER stress with accumulation of aggregated E-ZIKV proteins with disulfide-bond dependent polymers may contribute to congenital complications with neuronal disorders such

as microcephaly observed during Zika epidemics. Indeed, persistent ER stress can have deleterious effects on neuronal cell sensitivity to aggregated proteins in the short and medium terms of pregnancy and post-partum. This hypothesis could explain the occurrence of microcephaly in new-born babies several months after birth and mother's infection [40]. We therefore propose that these aggregates are likely of medical importance, as they could be one of the causative factors contributing to conformational diseases in neuronal cells. Further research into the proposed amyloid-like origin of ZIKV congenital complications is needed to investigate its suitability for targeted treatments of ZIKV infection.

Author Contributions: conceptualization, W.V., P.K.-T. ; methodology, J.T., E.F, W.V., P.K.-T.; validation, J.T., E.F, W.V., P.K.-T. ; formal analysis, J.T., E.F, C.E.K., P.D., W.V., P.K.-T. ; investigation, J.T., E.F, C.E.K.,W.V., P.K.-T. ; resources, P.D., W.V., P.K.-T.; data curation, J.T., E.F, P.D., W.V., P.K.-T.; writing—original draft preparation, J.T., E.F, P.D., W.V., P.K.-T.; writing—review and editing, J.T., E.F, P.D., W.V., P.K.-T.; visualization, W.V., P.K.-T.; supervision, W.V., P.K.-T.; project administration, P.D., W.V., P.K.-T.; funding acquisition,P.D.

Funding: This work was supported by the ZIKAlert project (European Union-Région Réunion program under grant agreement n° SYNERGY: RE0001902). E.F. holds a fellowship from the Regional Council of Reunion Island (European Union-Région Réunion program under grant agreement n° SYNERGY: RE0012406). J.T. has a PhD degree scholarship from La Réunion Island University (Ecole Doctorale STS), funded by the French ministry MEESR.

Acknowledgments: We thank the members of PIMIT and DéTROI laboratories for helpful discussions. We are grateful to Dr. Steeve Bourane and Dr. David A. Wilkinson for the critical review and improvements made to the use of the English language throughout the text. Also, Dr. Kazutoshi Mori, from Kyoto University, for providing us pGRP78-Luc and pGRP94-Luc plasmids.

Conflicts of Interest: The authors declare no conflict of interest.

References

1. Wen, Z.; Song, H.; Ming, G. How does Zika virus cause microcephaly? *Genes Dev.* **2017**, *31*, 849–861.
2. Miranda, J.; Martín-Tapia, D.; Valdespino-Vázquez, Y.; Alarcón, L.; Espejel-Nuñez, A.; Guzmán-Huerta, M.; Muñoz-Medina, J.E.; Shibayama, M.; Chávez-Munguía, B.; Estrada-Gutiérrez, G.; et al. Syncytiotrophoblast of Placentae from Women with Zika Virus Infection Has Altered Tight Junction Protein Expression and Increased Paracellular Permeability. *Cells* **2019**, *8*, 1174.
3. Cortese, M.; Goellner, S.; Acosta, E.G.; Neufeldt, C.J.; Oleksiuk, O.; Lampe, M.; Haselmann, U.; Funaya, C.; Schieber, N.; Ronchi, P.; et al. Ultrastructural Characterization of Zika Virus Replication Factories. *Cell Rep* **2017**, *18*, 2113–2123.
4. Miorin, L.; Romero-Brey, I.; Maiuri, P.; Hoppe, S.; Krijnse-Locker, J.; Bartenschlager, R.; Marcello, A. Three-dimensional architecture of tick-borne encephalitis virus replication sites and trafficking of the replicated RNA. *J. Virol.* **2013**, *87*, 6469–6481.
5. Romero-Brey, I.; Bartenschlager, R. Membranous Replication Factories Induced by Plus-Strand RNA Viruses. *Viruses* **2014**, *6*, 2826–2857.
6. Sun, Z.; Brodsky, J.L. Protein quality control in the secretory pathway. *J Cell Biol* **2019**, jcb.201906047.
7. Hendershot, L.M. The ER function BiP is a master regulator of ER function. *Mt. Sinai J. Med.* **2004**, *71*, 289–297.
8. Smith, J.A. A new paradigm: innate immune sensing of viruses via the unfolded protein response. *Front Microbiol* **2014**, *5*.

9. Carletti, T.; Zakaria, M.K.; Faoro, V.; Reale, L.; Kazungu, Y.; Licastro, D.; Marcello, A. Viral priming of cell intrinsic innate antiviral signaling by the unfolded protein response. *Nat Commun* **2019**, *10*, 3889.
10. Blázquez, A.-B.; Escribano-Romero, E.; Merino-Ramos, T.; Saiz, J.-C.; Martín-Acebes, M.A. Stress responses in flavivirus-infected cells: activation of unfolded protein response and autophagy. *Front Microbiol* **2014**, *5*.
11. Sano, R.; Reed, J.C. ER stress-induced cell death mechanisms. *Biochim. Biophys. Acta* **2013**, *1833*, 3460–3470.
12. Gardner, B.M.; Pincus, D.; Gotthardt, K.; Gallagher, C.M.; Walter, P. Endoplasmic reticulum stress sensing in the unfolded protein response. *Cold Spring Harb Perspect Biol* **2013**, *5*, a013169.
13. Almanza, A.; Carlesso, A.; Chintha, C.; Creedican, S.; Doultsinos, D.; Leuzzi, B.; Luís, A.; McCarthy, N.; Montibeller, L.; More, S.; et al. Endoplasmic reticulum stress signalling - from basic mechanisms to clinical applications. *FEBS J.* **2019**, *286*, 241–278.
14. Gladwyn-Ng, I.; Cordón-Barris, L.; Alfano, C.; Creppe, C.; Couderc, T.; Morelli, G.; Thelen, N.; America, M.; Bessières, B.; Encha-Razavi, F.; et al. Stress-induced unfolded protein response contributes to Zika virus-associated microcephaly. *Nat. Neurosci.* **2018**, *21*, 63–71.
15. Alfano, C.; Gladwyn-Ng, I.; Couderc, T.; Lecuit, M.; Nguyen, L. The Unfolded Protein Response: A Key Player in Zika Virus-Associated Congenital Microcephaly. *Front Cell Neurosci* **2019**, *13*, 94.
16. Hou, S.; Kumar, A.; Xu, Z.; Airo, A.M.; Stryapunina, I.; Wong, C.P.; Branton, W.; Tchesnokov, E.; Götte, M.; Power, C.; et al. Zika Virus Hijacks Stress Granule Proteins and Modulates the Host Stress Response. *J. Virol.* **2017**, *91*.
17. Amorim, R.; Temzi, A.; Griffin, B.D.; Mouland, A.J. Zika virus inhibits eIF2α-dependent stress granule assembly. *PLoS Negl Trop Dis* **2017**, *11*, e0005775.
18. Bonenfant, G.; Williams, N.; Netzband, R.; Schwarz, M.C.; Evans, M.J.; Pager, C.T. Zika Virus Subverts Stress Granules To Promote and Restrict Viral Gene Expression. *Journal of Virology* **2019**, *93*, e00520-19.
19. Monel, B.; Compton, A.A.; Bruel, T.; Amraoui, S.; Burlaud-Gaillard, J.; Roy, N.; Guivel-Benhassine, F.; Porrot, F.; Génin, P.; Meertens, L.; et al. Zika virus induces massive cytoplasmic vacuolization and paraptosis-like death in infected cells. *EMBO J.* **2017**, *36*, 1653–1668.
20. Umareddy, I.; Pluquet, O.; Wang, Q.Y.; Vasudevan, S.G.; Chevet, E.; Gu, F. Dengue virus serotype infection specifies the activation of the unfolded protein response. *Virol. J.* **2007**, *4*, 91.
21. Su, H.-L.; Liao, C.-L.; Lin, Y.-L. Japanese encephalitis virus infection initiates endoplasmic reticulum stress and an unfolded protein response. *J. Virol.* **2002**, *76*, 4162–4171.
22. Lee, Y.-R.; Kuo, S.-H.; Lin, C.-Y.; Fu, P.-J.; Lin, Y.-S.; Yeh, T.-M.; Liu, H.-S. Dengue virus-induced ER stress is required for autophagy activation, viral replication, and pathogenesis both in vitro and in vivo. *Sci Rep* **2018**, *8*, 1–14.
23. Peña, J.; Harris, E. Dengue virus modulates the unfolded protein response in a time-dependent manner. *J. Biol. Chem.* **2011**, *286*, 14226–14236.
24. Medigeshi, G.R.; Lancaster, A.M.; Hirsch, A.J.; Briese, T.; Lipkin, W.I.; Defilippis, V.; Früh, K.; Mason, P.W.; Nikolich-Zugich, J.; Nelson, J.A. West Nile virus infection activates the unfolded protein response, leading to CHOP induction and apoptosis. *J. Virol.* **2007**, *81*, 10849–10860.
25. Frumence, E.; Roche, M.; Krejbich-Trotot, P.; El-Kalamouni, C.; Nativel, B.; Rondeau, P.; Missé, D.; Gadea, G.; Viranaicken, W.; Desprès, P. The South Pacific epidemic strain of Zika virus replicates efficiently in human epithelial A549 cells leading to IFN-β production and apoptosis induction. *Virology* **2016**, *493*, 217–226.
26. El Kalamouni, C.; Frumence, E.; Bos, S.; Turpin, J.; Nativel, B.; Harrabi, W.; Wilkinson, D.A.; Meilhac, O.; Gadea, G.; Desprès, P.; et al. Subversion of the Heme Oxygenase-1 Antiviral Activity by Zika Virus. *Viruses* **2018**, *11*.
27. Viranaicken, W.; Nativel, B.; Krejbich-Trotot, P.; Harrabi, W.; Bos, S.; El Kalamouni, C.; Roche, M.; Gadea, G.; Desprès, P. ClearColi BL21(DE3)-based expression of Zika virus

antigens illustrates a rapid method of antibody production against emerging pathogens. *Biochimie* **2017**, *142*, 179–182.
28. Nozaki, J. ichi; Kubota, H.; Yoshida, H.; Naitoh, M.; Goji, J.; Yoshinaga, T.; Mori, K.; Koizumi, A.; Nagata, K. The endoplasmic reticulum stress response is stimulated through the continuous activation of transcription factors ATF6 and XBP1 in Ins2+/Akita pancreatic β cells. *Genes to Cells* **2004**, *9*, 261–270.
29. Mattioli, L.; Anelli, T.; Fagioli, C.; Tacchetti, C.; Sitia, R.; Valetti, C. ER storage diseases: a role for ERGIC-53 in controlling the formation and shape of Russell bodies. *Journal of Cell Science* **2006**, *119*, 2532–2541.
30. Beriault, D.R.; Werstuck, G.H. Detection and quantification of endoplasmic reticulum stress in living cells using the fluorescent compound, Thioflavin T. *Biochim. Biophys. Acta* **2013**, *1833*, 2293–2301.
31. Muñoz-Jordan, J.L.; Sánchez-Burgos, G.G.; Laurent-Rolle, M.; García-Sastre, A. Inhibition of interferon signaling by dengue virus. *Proc. Natl. Acad. Sci. U.S.A.* **2003**, *100*, 14333–14338.
32. Bos, S.; Viranaicken, W.; Turpin, J.; El-Kalamouni, C.; Roche, M.; Krejbich-Trotot, P.; Desprès, P.; Gadea, G. The structural proteins of epidemic and historical strains of Zika virus differ in their ability to initiate viral infection in human host cells. *Virology* **2018**, *516*, 265–273.
33. Turpin, J.; Frumence, E.; Desprès, P.; Viranaicken, W.; Krejbich-Trotot, P. The ZIKA Virus Delays Cell Death Through the Anti-Apoptotic Bcl-2 Family Proteins. *Cells* **2019**, *8*, 1338.
34. Saito, A.; Imaizumi, K. Unfolded Protein Response-Dependent Communication and Contact among Endoplasmic Reticulum, Mitochondria, and Plasma Membrane. *International Journal of Molecular Sciences* **2018**, *19*, 3215.
35. Limonta, D.; Jovel, J.; Kumar, A.; Airo, A.M.; Hou, S.; Saito, L.; Branton, W.; Ka-Shu Wong, G.; Mason, A.; Power, C.; et al. Human Fetal Astrocytes Infected with Zika Virus Exhibit Delayed Apoptosis and Resistance to Interferon: Implications for Persistence. *Viruses* **2018**, *10*.
36. Oka, O.B.V.; Bulleid, N.J. Forming disulfides in the endoplasmic reticulum. *Biochimica et Biophysica Acta (BBA) - Molecular Cell Research* **2013**, *1833*, 2425–2429.
37. Okamoto, T.; Suzuki, T.; Kusakabe, S.; Tokunaga, M.; Hirano, J.; Miyata, Y.; Matsuura, Y. Regulation of Apoptosis during Flavivirus Infection. *Viruses* **2017**, *9*.
38. Yoshida, H. ER stress and diseases. *The FEBS Journal* **2007**, *274*, 630–658.
39. Muneer, A.; Shamsher Khan, R.M. Endoplasmic Reticulum Stress: Implications for Neuropsychiatric Disorders. *Chonnam Med J* **2019**, *55*, 8–19.
40. van der Linden, V.; Pessoa, A.; Dobyns, W.; Barkovich, A.J.; Júnior, H. van der L.; Filho, E.L.R.; Ribeiro, E.M.; Leal, M. de C.; Coimbra, P.P. de A.; Aragão, M. de F.V.V.; et al. Description of 13 Infants Born During October 2015-January 2016 With Congenital Zika Virus Infection Without Microcephaly at Birth - Brazil. *MMWR Morb. Mortal. Wkly. Rep.* **2016**, *65*, 1343–1348.

Supplemental

Table 1. Cellular models of ZIKV infection and UPR activation.
nd= non determined

Figure S1. ZIKV inhibition by UPR activation. (A) A549 cells were infected with ZIKV at MOI of 5 for 18h. 2h post-infection TG or DTT were added at the indicated concentration. Cell mortality was evaluated through LDH release and absorbance measurement. **(B)** Viral progeny production in cell culture supernatants of cells infected and treated with TG or DTT were determined by PFU assay.